

## Article

# A Circularly Polarized Complementary Antenna with Substrate Integrated Coaxial Line Feed for X-Band Applications

Zhuoqiao Ji <sup>1</sup>, Guanghua Sun <sup>2</sup>, Kaixu Wang <sup>2</sup>, Hang Wong <sup>3,\*</sup>, Zhan Yu <sup>1</sup>, Zhengguo Li <sup>1</sup>, Changning Wei <sup>1</sup> and Pei Liu <sup>4,5</sup> 

<sup>1</sup> The Institute for Carbon-Neutral Technology, School of Automotive and Transportation Engineering, Shenzhen Polytechnic University, Shenzhen 518055, China; jizhuoqiao@szpu.edu.cn (Z.J.); yuzhan198423@szpu.edu.cn (Z.Y.); lizhengguo@szpu.edu.cn (Z.L.); weicn2023@szpu.edu.cn (C.W.)

<sup>2</sup> The School of Electronics and Information Engineering, Harbin Institute of Technology (Shenzhen), Shenzhen 518055, China; sunguanghua@hit.edu.cn (G.S.); wangkaixu@hit.edu.cn (K.W.)

<sup>3</sup> The State Key Laboratory of Terahertz and Millimeter Waves, Department of Electrical Engineering, City University of Hong Kong, Hong Kong 999077, China

<sup>4</sup> The School of Information Engineering, Wuhan University of Technology, Wuhan 430070, China; pei.liu@whut.edu.cn

<sup>5</sup> Zhongshan Institute of Advanced Engineering Technology, Wuhan University of Technology, Zhongshan 528437, China

\* Correspondence: hang.wong@cityu.edu.hk

**Abstract:** This work presents a design for a complementary antenna with circular polarization that has a wide operating bandwidth, stable broadside radiation, and stable gain for X-band applications. The proposed antenna consists of an irregular loop and a parasitic electric dipole, which work together to produce equivalent radiation from the magnetic and electric dipoles. By arranging the dipole and the loop in a specific geometry, this antenna effectively generates circularly polarized wave propagation. A substrate integrated coaxial line (SICL) is applied to feed the antenna through an aperture cutting on the ground. The proposed antenna achieves a wide axial ratio (AR) and impedance bandwidths of 27.4% (from 8.5 to 11.22 GHz, for the AR  $\leq$  3 dB) and 39.6% (from 7.5 to 11.2 GHz, for the reflection coefficient  $\leq$  -10 dB), respectively. Moreover, the antenna maintains a stable broadside radiation pattern across the operating bandwidth, with an average gain of 10 dBic. This proposed antenna design is competitive for X-band wireless communications.

**Keywords:** substrate integrated coaxial lines (SICL); wideband; circular polarization; complementary



**Citation:** Ji, Z.; Sun, G.; Wang, K.; Wong, H.; Yu, Z.; Li, Z.; Wei, C.; Liu, P.

A Circularly Polarized Complementary Antenna with Substrate Integrated Coaxial Line Feed for X-Band Applications.

*Electronics* **2024**, *13*, 785. <https://doi.org/10.3390/electronics13040785>

Academic Editor: Filippo Costa

Received: 31 December 2023

Revised: 8 February 2024

Accepted: 10 February 2024

Published: 17 February 2024



**Copyright:** © 2024 by the authors. Licensee MDPI, Basel, Switzerland. This article is an open access article distributed under the terms and conditions of the Creative Commons Attribution (CC BY) license (<https://creativecommons.org/licenses/by/4.0/>).

## 1. Introduction

Circularly polarized (CP) antennas are one of the important technologies in wireless communication applications. It is well known that the use of the CP wave is able to alleviate fading and the multipath effect and allows for flexibility in the orientation of the receiving and transmitting antennas. There are two conditions that should be satisfied to generate CP radiation, which are the generation of two orthogonal electric fields and the fact that the phase difference between these two orthogonal electric fields should reach 90 degree. Various other techniques have been introduced to produce CP radiation, such as a slot antenna with elliptic cavity [1], a water patch antenna with opposite truncated corners [2], and a semi-eccentric annular dielectric resonant antenna [3]. But, the 3-dB axial ratio (AR) bandwidths of these antennas [1–3] are smaller than 10%, which restricts their applications in wideband wireless communications. One of the traditional ways to generate CP radiation is by notching or truncating corners in the single-fed patch antenna to excite two orthogonal modes with a 90° phase difference. This kind of antenna has the merit of being low-profile, but its 3-dB AR bandwidth is typically narrow (less than 5%). The sequential rotation technique is then employed in the arrays of this kind of patch element to broaden both the impedance and the 3-dB AR bandwidths at the cost of enlarging the

antenna size [4–6]. The impedance bandwidth of the antenna array in [5] reached 31.9%, and the 3-dB AR bandwidth reached 21.56%. In Ref. [6], the antenna array achieved an impedance bandwidth of 36.3% and a 3-dB AR bandwidth of 20.4%. To further enhance the bandwidth, a cross-dipole antenna with eight parasitic shorted patches was proposed in [7], which achieved a 61.8% –10-dB impedance bandwidth and a 51.6% 3-dB AR bandwidth, but its antenna gain was less than 5 dBic. Some researchers used the magneto-electric (ME) dipole to design the CP antennas due to its wide bandwidth and stable radiation pattern. In Ref. [8], a CP ME dipole antenna using the *L*-probe feed obtained 56.7% impedance bandwidth and 41% 3-dB AR bandwidth. However, the antenna's performance is sensitive to the *L*-probe structure. To address this problem, Ref. [9] proposed a CP magneto-electric (ME) dipole antenna with an aperture-coupled feed, which obtained an impedance and AR bandwidth of 58.2% and 22.5%, respectively. Though the CP antennas in [8,9] have a wide AR and impedance bandwidth, their maximum gains are difficult to obtain when higher than 10 dBic. CP antenna designs with dielectric rod are good choices to achieve high gain and wideband performances [10–12]. A dielectric rod antenna is surface-wave antenna, and the linearly-polarized antenna designs usually have wide impedance bandwidth, which makes it a good candidate in designing CP antennas. The antenna design in [10] made use of a helix antenna to excite the dielectric rod. The AR bandwidth achieved is about 22%. However, the antenna structure is complicated due to the utilization of a helix antenna. In Ref. [11], CP radiation of the dielectric rod antenna was achieved by rotating the matching taper to 45 degrees relative to the radiation taper, the 3-dB AR bandwidth of which is about 37%. Meanwhile, the impedance matching is all below –10 dB throughout the Ka band. The averaged gain is around 9 dBic. The antenna design in [12] uses a complementary CP source, the impedance bandwidth is about 52.9%, and the 3-dB AR bandwidth is about 42%. The maximum antenna gain achieved is about 12.9 dBic. Lens antennas are also strong competitors in high-gain and wideband CP antenna designs. In Ref. [13], the antenna structure is composed of several slabs in air or in a dielectric to transform the linear polarization into circular polarization. The impedance bandwidth achieved is 50%, with a 30% overlapped 3-dB AR bandwidth. The maximum antenna gain is about 15 dBic. In Ref. [14], the integration of the dielectric polarizer and the hemispherical dielectric lens further enhances the antenna gain to about 21.4 dBic. The impedance bandwidth and 3-dB AR bandwidth achieved are about 27% and 29%, respectively. Though the CP dielectric rod antennas and lens antennas have the benefits of high gain and wide bandwidth, they suffer from a high antenna profile and a bulky antenna structure. Therefore, studies of high-gain, wideband, and low-profile antennas are in demand.

The idea of the complementary antenna was first adopted by Chlavin in the year 1954 [15]. The radiation patterns of the electric dipole (*E*-dipole) in *E*- and *H*-planes are in figure "8" shape and figure "O" shapes, while the radiation patterns of the magnetic dipole (*M*-dipole) in *E*- and *H*-planes are complementary to the *E*-dipole. By properly designing the *E*-dipole and the *M*-dipole, equal radiation patterns in both *E*- and *H*-planes with low backward radiation can be achieved. In the year 1960, Owyang and King presented a complementary antenna constructed using a slot and a pair of dipoles located symmetrically between the slot [16]. The current distribution of the slot and the dipoles were analyzed, and their relationship was discussed. After decades, in [17], Luk and Wong proposed a complementary antenna composed of an *E*-dipole and an *M*-dipole, and it was named the "ME dipole antenna." It possessed the characteristics of wide bandwidth, stable antenna gain, and low backward radiation. People then started to pay more attention to complementary antenna designs. In Ref. [18], a patch-slot dipole antenna with a backed cavity was proposed for millimeter-wave CP applications, which achieved an impedance bandwidth of 14.5% and a 3-dB AR bandwidth of 15.7%. A CP complementary antenna for 60 GHz applications was proposed in [19], and the overlapping bandwidth was enlarged to 21.9%. Lin proposed an omnidirectional CP antenna with 8% overlapping bandwidth for 5G cellular system and well explained the operating principle of the CP complementary antenna [20]. In Ref. [21], a wideband CP endfire antenna based on a complementary dipole

was proposed, and the impedance and 3-dB AR bandwidth achieved were 51.1% and 25%, respectively. In Ref. [22], a wideband CP complementary antenna with a simple structure was proposed with an impedance bandwidth of 32.7% and a 3-dB AR bandwidth of 30.9%. However, the maximum antenna gain achieved was 7.95 dBic.

In this article, we present a high-gain and low-profile CP complementary antenna with an aperture-coupled feed, which is composed of an irregular loop that produces *M*-dipole radiation and a parasitic dipole that produces *E*-dipole radiation. The antenna feed is a substrate integrated coaxial line (SICL), which is a low-dispersive structure first proposed in [23] and then applied in [24–26]. The sandwich structure of SICL effectively reduces the dispersion of the microstrip line and helps to suppress backlobe radiation. Moreover, the SICL has the advantage of design flexibility compared with the waveguide or the substrate integrated waveguide (SIW).

The measured results show that the antenna is able to achieve an average gain of 10 dBic with a low profile of  $0.125 \lambda_0$  ( $\lambda_0$  is one wavelength in the free space at the center frequency of 9.35 GHz). The antenna impedance bandwidth and the 3-dB AR bandwidth are 39.6% (from 7.5 to 11.22 GHz) and 27.4% (8.5 to 11.22 GHz), respectively. The proposed antenna design could be a competitive design for wireless communication in X-band applications.

## 2. Antenna Design

The paralleled *M*-dipole and *E*-dipole radiations can generate two electric fields with orthogonal directions such that the  $90^\circ$  phase difference is naturally achieved when the *M*- and *E*-dipoles are in-phase fed by the same source [18–22]. With this inspiration, a CP complementary dipole antenna is proposed and shown in Figure 1. The radiator consists of a parasitic dipole and an irregular loop formed by a patch in an S shape with two vertical strip lines in pairs excited by an aperture cut on the ground. The parasitic dipole generates an electric dipole radiation, while the irregular loop produces a magnetic dipole radiation. By carefully designing the geometry of the dipole and loop, a pair of orthogonal electric fields is generated, resulting in CP radiation across a wide bandwidth. To be comprehensible, the parasitic dipole (in red) and the irregular loop (in purple) are independently shown in Figure 1e. As the vertical strip lines are differentially fed by the slot, they can be considered to be connected with each other. With the integration of the S-shaped patch and the vertical strip lines, the structure can be regarded as a folded irregular loop antenna. As the loop antenna can be considered a magnetic dipole, the irregular loop structure can be regarded as a magnetic dipole. The parasitic dipole and the irregular loop are all diagonally placed, and the relevant electric dipole and magnetic dipole are paralleled to each other; therefore, CP radiation is generated. The methodology of the proposed antenna design involves utilization of the complementary antenna theory. As analyzed in [18–22], the parallelly placed *M*-dipole and *E*-dipole can generate two orthogonal electric fields with a  $90^\circ$  phase difference; therefore, the two conditions of generating CP radiation are satisfied. In the proposed antenna design, the parasitic dipole is placed in a diagonal direction, and it produces *E*-dipole radiation. The irregular loop is placed in a diagonal direction, and it produces *M*-dipole radiation. Therefore, the constructed *E*-dipole and *M*-dipole are all along the diagonal direction and paralleled to each other. In this case, the complementary antenna theory can be applied in this antenna design, and circular polarization is generated.

To excite the antenna, a Y-shaped power divider was constructed using an SICL is proposed. The feeding network is a two-layer sandwich structure, with the Y-shaped microstrip line on the top of Substrate 1 being shielded by the metallic vias through Substrate 1 and Substrate 2. A slot cut on the top surface of Substrate 2 is fed by the Y-shaped microstrip line and works as the feed of the radiator. A copper ground with an etched slot is placed between the feeding network and the radiator as a connection so that the radiator can be soldered in its exact position. A commercial EM simulator, Ansoft HFSS, was used in the simulation of the proposed antenna. In this work, Rogers 5880 is used to design the proposed antenna, the relative dielectric constant of which is 2.2. The substrate

thicknesses of Substrate 1 and Substrate 2 are 0.787 mm and 0.381 mm, respectively. The copper thickness of the ground and the radiator are 0.3 mm and 0.8 mm, respectively. The height of the radiator  $H_r$  is 4 mm, which is only a 0.125 wavelength at 9.35 GHz in free space. The proposed antenna dimensions are listed in Table 1 in detail.

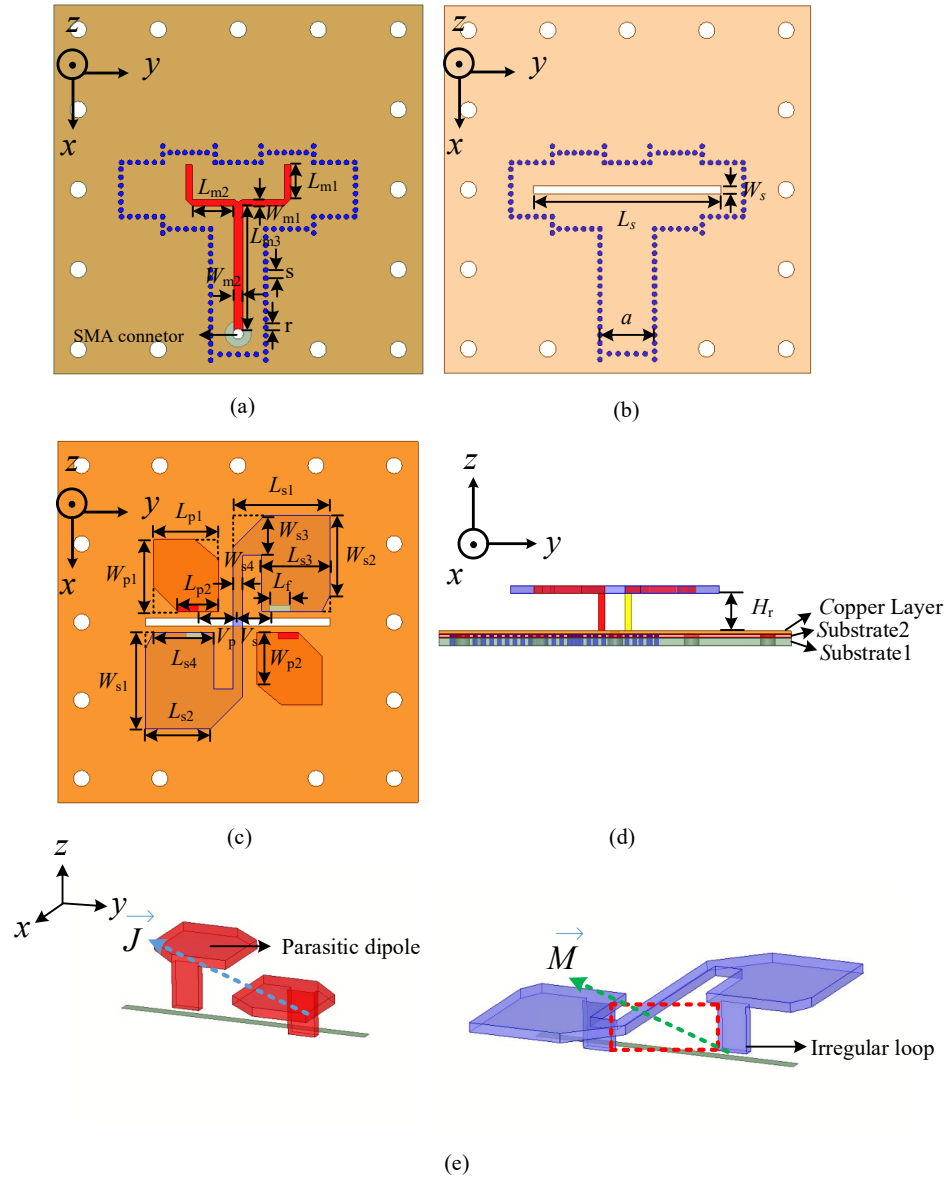


**Figure 1.** Geometry of the proposed antenna element: (a) top view of Substrate 1; (b) top view of Substrate 2; (c) top view of the copper layer and the radiator; (d) side view; (e) exploded view.

**Table 1.** Parameters of the proposed antenna (unit: mm).

| Para.    | Value | Para.    | Value | Para.    | Value |
|----------|-------|----------|-------|----------|-------|
| $L_{m1}$ | 4.2   | $a$      | 6.7   | $L_{s1}$ | 12.1  |
| $L_{m2}$ | 5.05  | $L_s$    | 23    | $L_{s2}$ | 7.1   |
| $L_{m3}$ | 15.25 | $W_s$    | 1     | $L_{s3}$ | 8.5   |
| $W_{m1}$ | 0.8   | $L_{p1}$ | 8.1   | $L_{s4}$ | 7.5   |
| $W_{m2}$ | 1.1   | $L_{p2}$ | 5.1   | $W_{s1}$ | 12    |
| $s$      | 1     | $W_{p1}$ | 9     | $W_{s2}$ | 9.5   |
| $r$      | 0.3   | $W_{p2}$ | 6     | $W_{s3}$ | 5     |
| $V_p$    | 5     | $V_s$    | 4     | $L_f$    | 2.5   |
| $H_r$    | 4     | $W_{s3}$ | 1.2   |          |       |

### 3. Antenna Analysis and Parametric Study

#### 3.1. Antenna Analysis

To better illustrate the antenna operating principle, the proposed antenna current distribution at 9 GHz over one cycle of time is shown in Figure 2. It shows that at the moment of  $t = 0$  and  $t = T/2$ , the currents on the truncated patch, which is considered the  $E$ -dipole and the  $S$ -shaped patch, which forms the  $M$ -dipole, are along the diagonal direction and the  $y$  axis, while at the time  $t = T/4$  and  $t = 3T/4$ , the current on the truncated patch is along the diagonal direction, and on the  $S$ -shaped patch, it is along the  $x$  direction. Therefore, two electric fields in orthogonal directions with  $T/4$  delay time ( $90^\circ$  phase difference) are generated. The currents are rotated in an anti-clockwise direction, which indicates that the proposed antenna has a right-hand circular polarization (RHCP) radiation.

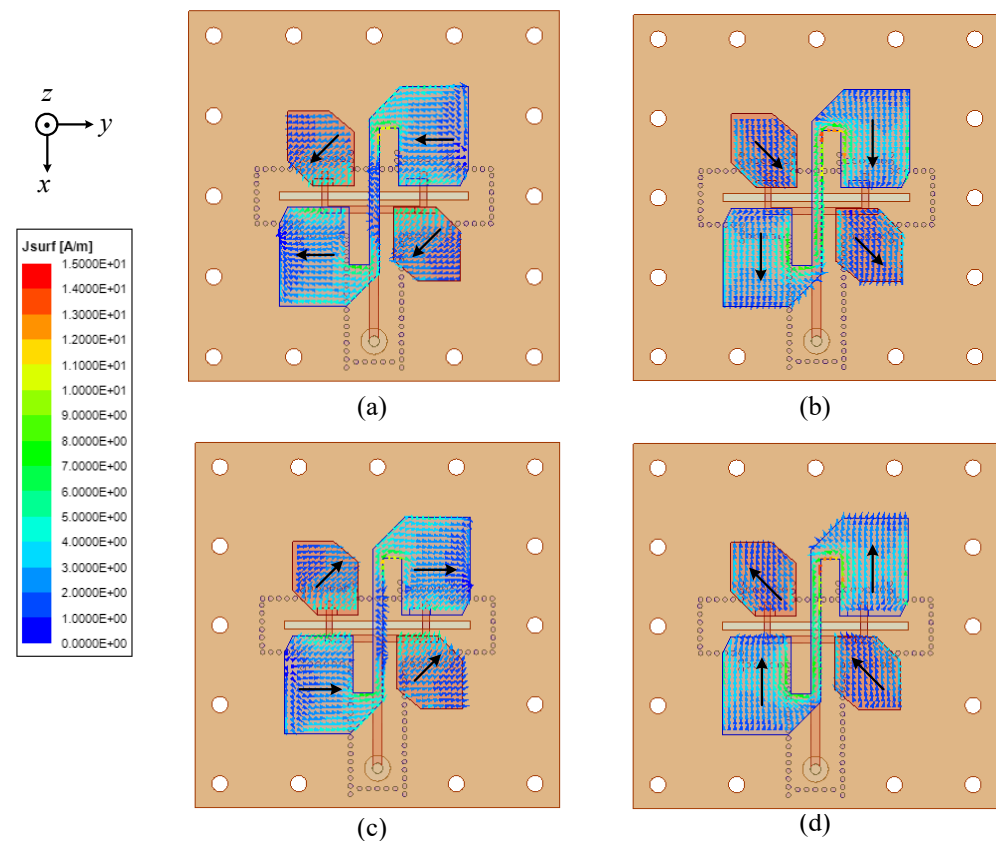


**Figure 2.** The proposed antenna current distribution at 9 GHz over one cycle of time: (a)  $t = 0$ ; (b)  $t = T/4$ ; (c)  $t = T/2$ ; (d)  $t = 3T/4$ .

To distinguish the importance of employing the SICL structure, comparisons of the front-to-back ratio and antenna gain between the antenna designs with and without the SICL structure were carried out, as shown in Figures 3 and 4. In Figure 3, it shows that when removing the SICL structure (the ground plane at the bottom of Substrate 1 is also removed), the front-to-back ratio deteriorates dramatically. As the antenna feed of the radiator is a slot, which is a bidirectional radiating structure, the backward radiation is inescapable unless a reflector is placed under the slot. In this antenna design, a ground plane is placed under the Y-shaped microstrip line, and it acts as a reflector to reduce the backward radiation. However, as the microstrip line is dispersive and has radiation loss, the front-to-back ratio performance of the antenna is affected if the microstrip line is unshielded. From Figure 3, it is clearly shown that the antenna design with the SICL structure is superior to the one without the SICL structure, which has around 10 dB of enhancement in terms of the front-to-back ratio performance. From Figure 4, it shows that the antenna gain is more stable when using the SICL structure. Moreover, the antenna

gain is greatly enhanced due to the utilization of the SICL structure. The reason for this enhancement is that the Y-shaped microstrip line is shielded by the metallic vias, which reduce the dispersion and radiation loss [18]. The sandwich structure of the SICL shows its advantages in improving the front-to-back ratio and antenna gain when compared with the microstrip line unshielded.

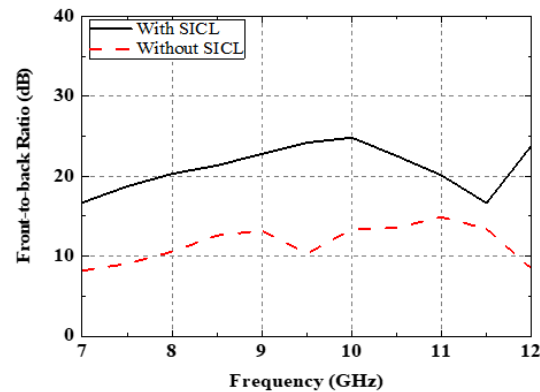


**Figure 3.** Comparison of the front-to-back ratio between the antenna designs with and without the SICL.

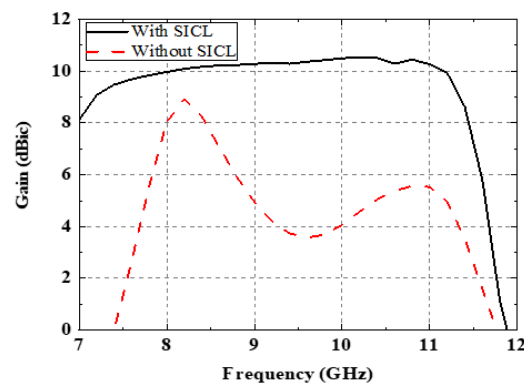


**Figure 4.** Comparison of the antenna gain between the antenna designs with and without the SICL.

### 3.2. Parametric Study

A series of studies on the parameters was conducted to investigate and provide a guideline for the proposed antenna design. Every time, only the investigated parameter was changed, while the rest of the parameters were the same, as shown in Table 1.

Figure 5 shows the parametric study results of  $L_{m2}$ . The value of  $L_{m2}$  has a significant influence on the antenna impedance performance because it determines the length of the microstrip feeding line and the feeding position on the slot. From Figure 5a, it is shown that the reflection coefficient has a large variation as the value of  $L_{m2}$  changes. The value of  $L_{m2}$  has a limited influence on the field distribution of the radiator because the microstrip line is shielded by the metallic ground plane. Therefore, the antenna AR slightly changes under different values of  $L_{m2}$ .

The parametric study results of  $W_{s1}$  are plotted in Figure 6. The value of  $W_{s1}$  dictates the size of the S-shaped patch or the M-dipole. The radiation impedance of the antenna and the radiation phase of the M-dipole are different when the  $W_{s1}$  value changes. Consequently, the  $W_{s1}$  affects the reflection coefficient and the antenna AR as well. From Figure 6a, it shows that the best impedance matching is obtained when  $W_{s1}$  equals to 12 mm. A deviation from this value causes a degradation to the impedance matching. A resonance mode, where the AR is very small, can be generated at a high frequency by carefully adjusting the value of  $W_{s1}$ , as shown in Figure 6b. When the  $W_{s1}$  is too large, the resonance mode moves to a lower frequency, which leads to a narrow AR bandwidth, as shown in the

case of  $W_{s1} = 14$  mm. And, the AR becomes worse within the operating band when the  $W_{s1}$  is too small. When  $W_{s1}$  equals 12 mm, the antenna achieves a wide AR bandwidth.

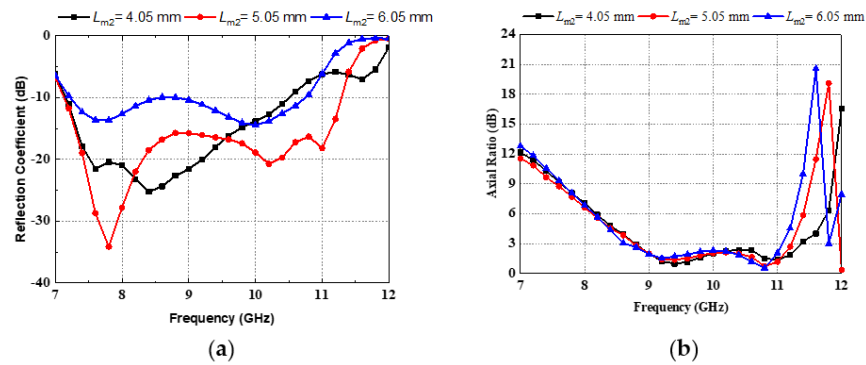


Figure 5. Parametric study of  $L_{m2}$ . (a) Reflection coefficient. (b) Axial ratio.

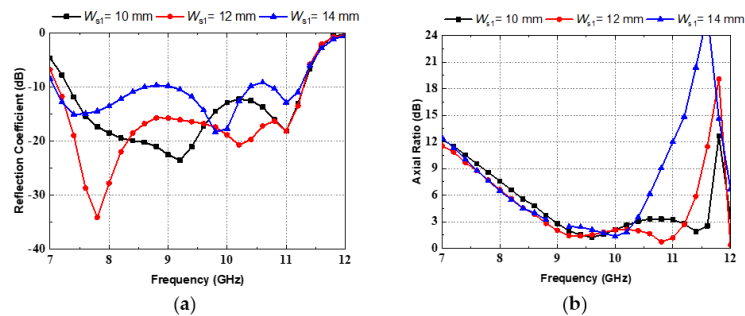


Figure 6. Parametric study of  $W_{s1}$ . (a) Reflection coefficient. (b) Axial ratio.

The feeding position of the S-shaped patch (the location of the vertical strip lines) was studied, as shown in Figure 7. From Figure 7a, it shows that the value of  $V_s$  mainly affects the second resonant frequency. As  $V_s$  increases, the second resonant frequency shifts to a lower frequency. Figure 7b shows that at around 9.5 GHz, the AR value increases as  $V_s$  increases. The antenna height  $H_r$  is studied in Figure 8. The impedances of the  $M$ - and the  $E$ -dipoles are varied under different  $H_r$ . However, only a slight variation of the reflection coefficient is found, as shown in Figure 8a. Because the proposed antenna is constituted by the  $M$ -dipole and the  $E$ -dipole, its impedance bandwidth would be inherently wide. Therefore, the reflection coefficient remains stable as the height of the antenna changes. Nonetheless, the  $H_r$  has an obvious influence on the AR performance, as shown in Figure 8b. The value of  $H_r$  affects the phases of both electric fields from the  $M$ -dipole and the  $E$ -dipole such that the AR response would be much varied.

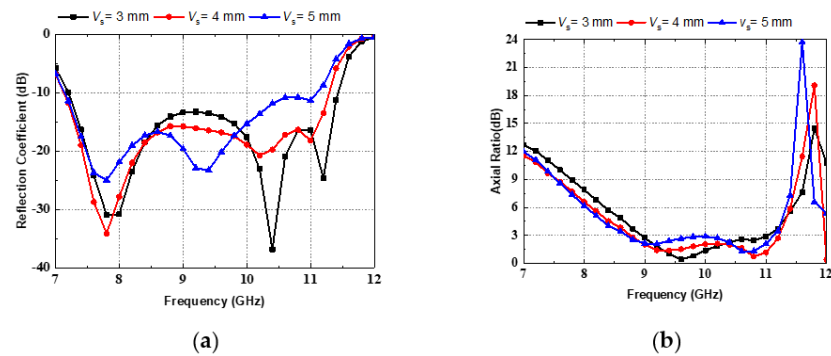
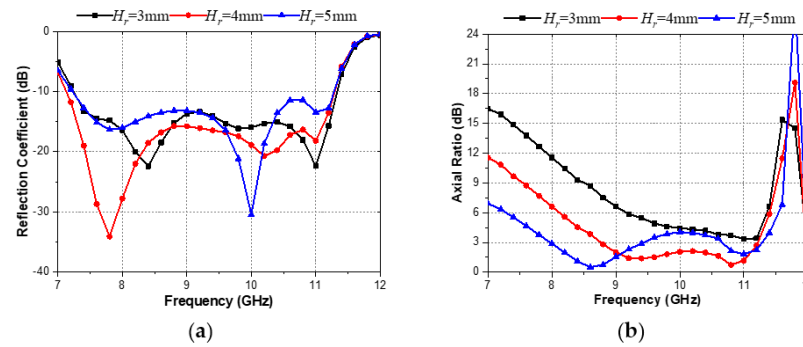


Figure 7. Parametric study of  $V_s$ . (a) Reflection coefficient. (b) Axial ratio.



**Figure 8.** Parametric study of  $H_r$ . (a) Reflection coefficient. (b) Axial ratio.

## 4. Measured Results and Discussion

### 4.1. Measurement Results

Fabrication and measurement were performed to verify the proposed antenna performance. Figure 9 shows the photography of two substrates and the copper layer, as well as the assembled prototype. The antenna reflection coefficients and the gains are shown in Figure 10. The simulated and measured gains are in agreement. The simulation and measurement results of the reflection coefficients have discrepancies due to the fabrication errors, as well as the alignment error and the air gaps between Substrate 1 and Substrate 2. The simulation and measurement results of the ARs are displayed in Figure 11. The 3-dB AR bandwidth measured is 27.4% from 8.5 to 11.2 GHz. The average gain of 10 dBic was obtained across the operating bandwidth. It should be mentioned that the proposed antenna has some limitations in the fabrication and the assembly of the antenna. The fabrication has to be separated into the substrate parts and the metal parts. Therefore, two factories have to be found to perform the relevant fabrications. Moreover, the parasitic patch and the S-shaped patch with vertical strip lines have to be soldered separately in the ground plane. This affects the accuracy of the fabrications, increases the difficulty in assembling the antenna, and causes discrepancies between the simulation and the measurement results.

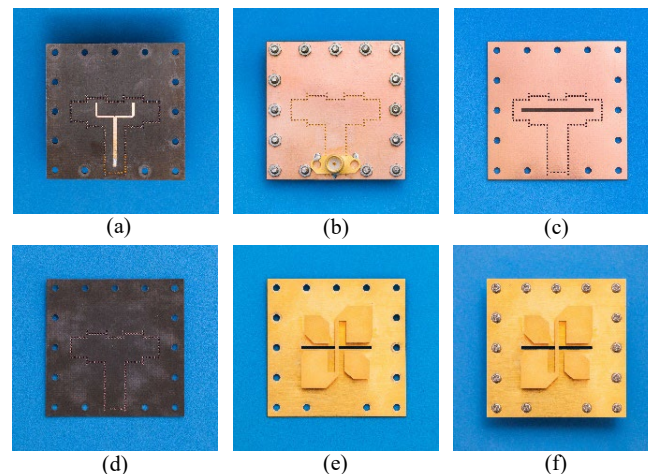


**Figure 9.** Fabricated prototype of the proposed antenna. (a) Top view of Substrate 1. (b) Bottom view of Substrate 1. (c) Top view of Substrate 2. (d) Bottom view of Substrate 2. (e) Top view of the copper layer. (f) Top view of the assembled antenna.

The radiation patterns in the two planes of the  $XoZ$  and  $YoZ$  planes are shown in Figure 12. The antenna achieves a stable RHCP radiation pattern with a low side lobe and backlobe. The cross-polarization discriminations are kept within  $-15$  dB in regard to the polar angle from  $-30^\circ$  to  $30^\circ$ . The front to back ratios of the radiation patterns are greater than 20 dB on both planes for the three selected frequencies.

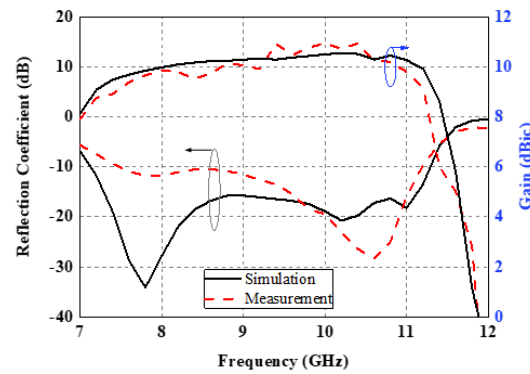


Figure 10. Simulated and measured reflection coefficients and gains of the proposed antenna.

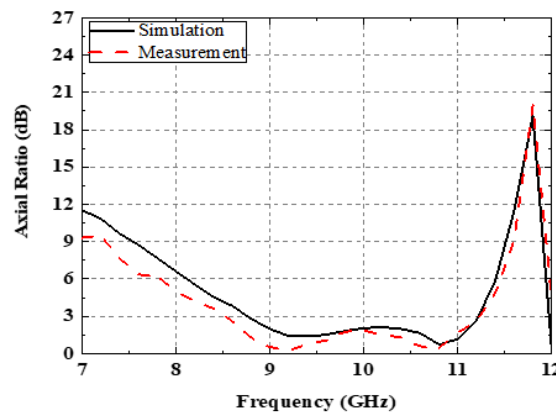
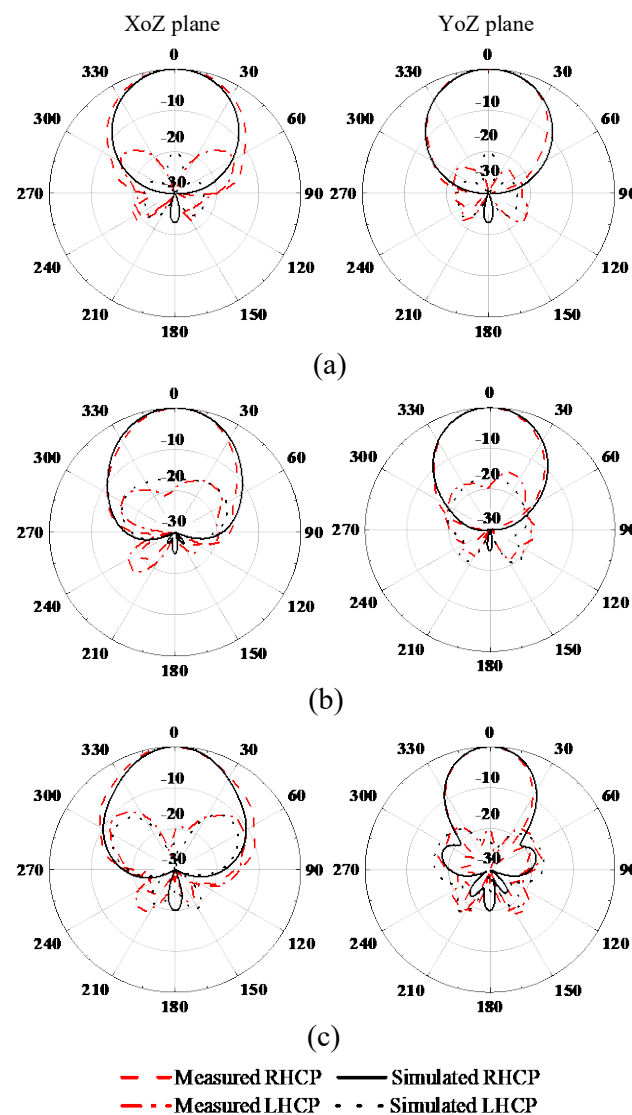


Figure 11. Simulated and measured AR of the proposed antenna.

#### 4.2. Discussion

Compared with the published works regarding CP antenna designs, this work finds its superiority in terms of the stable high antenna gain, which reaches over 10 dBic (the gain variation is smaller than 0.6 dBic) in the operating bandwidth, low backlobe and cross-polarization level, and low profile, which is only a 0.125 wavelength at 9.35 GHz in free space, as well as the wide impedance and AR bandwidth. The comparison of the proposed antenna and the reported CP antenna designs with detailed information is shown in Table 2. For the design proposed in [7], the impedance bandwidth and 3-dB AR bandwidth are 61.8% and 51.6%, respectively. However, its antenna gain is less than 5 dBic. For the design in [8], though its impedance bandwidth and 3-dB AR bandwidth reach 56.7% and 41%, respectively, the antenna gain varies from 5 to 9.9 dBic, and its antenna height is around a 0.15 wavelength in the free space referring to the center frequency, while in this work the antenna height is only a 0.125 wavelength at 9.35 GHz in free space. For the design proposed in [18], though the maximum antenna gain reaches 10 dBic, the antenna gain across the operating bandwidth is not stable, and it has a variation of more than 2 dBic. Moreover, its impedance and 3-dB AR bandwidth are only 14.5% and 15.7%, respectively. In [19], the overlapping bandwidth achieved reaches 21.9%. In this work, the impedance and 3-dB AR bandwidth achieved are 39.6% and 27.4%, respectively. For the design in [22], though it achieves an impedance bandwidth of 32.7% and a 3-dB AR bandwidth of 30.9%, its maximum antenna gain is only 7.95 dBic. It can be seen from Table 2 that the antenna gain is stable with a gain variation smaller than 0.6 dBic across the operating band. For the designs in [8,18], a probe is used to feed the antenna, and therefore they suffer from a high cross-polarization problem. The backlobe level of the designs in [7,22] is high. For [7], it is due to the use of the parasitic shorted elements, and for [22], it uses a slot as the antenna feed. In the proposed antenna design, the SICL is used to deal with the high backlobe problem introduced by the slot feed. It can be seen from Table 2 that the proposed antenna design achieves low backlobe and a low cross-polarization level at the same time.

Therefore, for the overall consideration, including the operating bandwidth, the maximum antenna gain, the gain stability, the antenna profile, the backlobe, and the cross-polarization level, the proposed antenna design is a competitive candidate for CP antenna designs. The measurement results of the proposed antenna design have discrepancies compared with the simulation result. This is due to the unavoidable fabrication errors, as well as the alignment error and the air gaps between Substrate 1 and Substrate 2. As the thicknesses of the substrates used in this work are only 0.787 mm and 0.381 mm, they bend after fabrication. Though screws are used to combine the substrates together, air gaps between the substrates still exist. Therefore, the measurement results of the proposed antenna are affected to some extent. It is suggested to use two thick metallic blocks to compress the substrates before assembling the antenna when designing similar antenna structures.



**Figure 12.** Simulation and measurement results of radiation patterns for the proposed antenna at: (a) 9 GHz; (b) 10 GHz; (c) 11 GHz.

The superiority of the proposed antenna design compared with other complementary antenna designs is mainly attributed to the utilization of the SICL feeding structure and the irregular loop, which is composed of a patch in an S shape with two vertical strip lines in pairs. The SICL feeding structure helps to achieve a high and stable antenna gain as well as a low backlobe level, while the S-shaped patch is beneficial for enhancing the flexibility of the antenna structure in optimizing the impedance matching and the AR performance of

the proposed antenna. As the S-shaped patch is constructed using fragments of different sizes, changing the length and width of the fragments has an influence on the performance of the impedance matching and the AR.

**Table 2.** Comparison of the proposed antenna and the reported CP antenna designs.

| Ref.      | Antenna Type            | Imp. BW (%) | ARBW (%) | Max. Gain (dBic) | Gain Variation (dBic) | Height           | Backlobe (dB) | Cross-Polarization (dB) |
|-----------|-------------------------|-------------|----------|------------------|-----------------------|------------------|---------------|-------------------------|
| [7]       | Cross-dipole            | 61.8        | 51.6     | 4.03             | <2                    | $0.067\lambda_0$ | −6            | −16                     |
| [8]       | Magneto-electric dipole | 56.7        | 41       | 9.9              | 4.9                   | $0.15\lambda_0$  | −22           | −10                     |
| [18]      | Patch-slot dipole       | 14.5        | 15.7     | 11.2             | 3.2                   | $0.1\lambda_0$   | −25           | −10                     |
| [19]      | Complementary antenna   | 23.8        | 23.4     | 8.6              | 3.3                   | $0.15\lambda_0$  | −20           | −10                     |
| [22]      | Complementary antenna   | 32.7        | 30.9     | 7.95             | 2.5                   | $0.21\lambda_0$  | −8            | −5                      |
| This work | Complementary antenna   | 39.6        | 27.4     | 10.5             | 0.6                   | $0.125\lambda_0$ | −25           | −16                     |

The data of the backlobe and cross-polarization level in the table are according to the center frequency of the operating band.

## 5. Conclusions

In this work, a wideband CP complementary antenna has been presented for X-band applications. A SICL structure was applied as the feed for the purpose of wide antenna impedance matching and low backlobe radiation. The radiator comprises a parasitic dipole and a loop, which act as the *E*- and *M*-dipoles, respectively. Wideband RHCP radiation was realized by controlling the phase distribution of the *M*- and *E*-dipoles. The measurement results show that the antenna design proposed can obtain a 39.6% impedance bandwidth and a 27.4% 3-dB AR bandwidth with an average gain of 10 dBic. With a wide operating band and stable radiation patterns, the CP antenna design proposed has potential applications in X-band wireless communications, such as satellite applications (wireless broadcast satellite applications and weather satellite applications) and aerospace communication.

**Author Contributions:** Conceptualization, H.W. and Z.L.; methodology, Z.J. and G.S.; software, Z.J. and K.W.; validation, Z.J. and G.S.; formal analysis, Z.J. and K.W.; investigation, Z.J., Z.Y., C.W., and P.L.; writing—original draft preparation, Z.J. and G.S.; writing—review and editing, H.W. and K.W. All authors have read and agreed to the published version of the manuscript.

**Funding:** This work was supported in part by the Guangdong Basic and Applied Basic Research Foundation under Grant 2022A1515110083, the Shenzhen Basic Research Program under Grant GXWD20220811163824001, the Shenzhen Science and Technology Innovation Commission under Grant RCBS20221008093123059, the Shenzhen Humanities & Social Sciences Key Research Bases, the National Key Research and Development Program of China (No. 2020YFB1807300), the National Natural Science Foundation of China under Grant 62001140, the Shenzhen Basic Research Program under Grant GXWD20201230155427003-20200824201212001, the Open Research Project of the Guangdong Provincial Key Laboratory of Millimeter-Wave and Terahertz (No. 2019B030301002KF2002), and the Shenzhen Science and Technology Program under Grant KQTD20210811090116029. The work of Pei Liu was supported in part by the National Natural Science Foundation of China under Grant 62001336, the Knowledge Innovation Program of Wuhan-Shuguang Project under Grant 2023010201020316, the Guangdong Basic and Applied Basic Research Foundation, and the China Scholarship Council (CSC) under Grant 202306950052.

**Data Availability Statement:** All of the data are contained within the article.

**Conflicts of Interest:** All authors declare no conflicts of interest.

## References

- Xu, Y.; Wang, Z.; Dong, Y. Circularly Polarized Slot Antennas with Dual-Mode Elliptical Cavity. *IEEE Antennas Wirel. Propag. Lett.* **2020**, *19*, 715–719. [\[CrossRef\]](#)
- Sun, J.; Luk, K.-M. A Circularly Polarized Water Patch Antenna. *IEEE Antennas Wirel. Propag. Lett.* **2020**, *19*, 926–929. [\[CrossRef\]](#)
- Lee, J.M.; Kim, S.-J.; Kwon, G.; Song, C.M.; Yang, Y.; Lee, K.-Y.; Hwang, K.C. Circularly Polarized Semi-Eccentric Annular Dielectric Resonator Antenna for X-Band Applications. *IEEE Antennas Wirel. Propag. Lett.* **2015**, *14*, 1810–1813. [\[CrossRef\]](#)

4. Hall, P.S.; Dahele, J.S.; James, J.R. Design principles of sequentially fed, wide bandwidth, circularly polarised microstrip antennas. *IEE Proc. H Microw. Antennas Propag.* **1989**, *136*, 381–389. [[CrossRef](#)]
5. Ta, S.X.; Park, I. Compact Wideband Sequential-Phase Feed for Sequentially Rotated Antenna Arrays. *IEEE Antennas Wirel. Propag. Lett.* **2016**, *16*, 661–664. [[CrossRef](#)]
6. Sun, M.; Liu, N.; Zhu, L.; Fu, G. Wideband circularly polarized sequentially rotated microstrip antenna array with sequential-phase feeding network. *J. Commun. Inf. Netw.* **2020**, *5*, 350–357. [[CrossRef](#)]
7. Yang, W.-J.; Pan, Y.-M.; Zheng, S.-Y. A Compact Broadband Circularly Polarized Crossed-Dipole Antenna with a Very Low Profile. *IEEE Antennas Wirel. Propag. Lett.* **2019**, *18*, 2130–2134. [[CrossRef](#)]
8. Li, M.; Luk, K.-M. A Wideband Circularly Polarized Antenna for Microwave and Millimeter-Wave Applications. *IEEE Trans. Antennas Propag.* **2014**, *62*, 1872–1879. [[CrossRef](#)]
9. Sun, J.; Luk, K.-M. Wideband Linearly-Polarized and Circularly-Polarized Aperture-Coupled Magneto-Electric Dipole Antennas Fed by Microstrip Line With Electromagnetic Bandgap Surface. *IEEE Access* **2019**, *7*, 43084–43091. [[CrossRef](#)]
10. Hui, H.; Ho, Y.; Yung, E. A cylindrical DR rod antenna fed by a short helix. In Proceedings of the IEEE Antennas and Propagation Society International Symposium, 1996 Digest, Baltimore, MD, USA, 21–26 July 1996; Volume 3, pp. 1946–1949.
11. Ji, Z.; Wang, K.X.; Wong, H. Circularly Polarized Dielectric Rod Waveguide Antenna for Millimeter-Wave Applications. *IEEE Trans. Antennas Propag.* **2018**, *66*, 5080–5087. [[CrossRef](#)]
12. Wang, J.; Li, Y.; Ge, L.; Wang, J.; Chen, M.; Zhang, Z.; Li, Z. Millimeter-Wave Wideband Circularly Polarized Planar Complementary Source Antenna with Endfire Radiation. *IEEE Trans. Antennas Propag.* **2018**, *66*, 3317–3326. [[CrossRef](#)]
13. Wang, K.X.; Wong, H. A Wideband Millimeter-Wave Circularly Polarized Antenna With 3-D Printed Polarizer. *IEEE Trans. Antennas Propag.* **2017**, *65*, 1038–1046. [[CrossRef](#)]
14. Wang, K.X.; Wong, H. Design of a Wideband Circularly Polarized Millimeter-Wave Antenna with an Extended Hemispherical Lens. *IEEE Trans. Antennas Propag.* **2018**, *66*, 4303–4308. [[CrossRef](#)]
15. Chlavin, A. A new antenna feed having equal E- and H-plane patterns. *Trans. IRE Prof. Group Antennas Propag.* **1954**, *2*, 113–119. [[CrossRef](#)]
16. King, R.; Owyang, G. The slot antenna with coupled dipoles. *IRE Trans. Antennas Propag.* **1960**, *8*, 136–143. [[CrossRef](#)]
17. Luk, K.M.; Wong, H. A new wideband unidirectional antenna element. *Int. J. Microw. Opt. Technol.* **2006**, *1*, 35–44.
18. Bai, X.; Qu, S.-W.; Ng, K.B. Millimeter-Wave Cavity-Backed Patch-Slot Dipole for Circularly Polarized Radiation. *IEEE Antennas Wirel. Propag. Lett.* **2013**, *12*, 1355–1358. [[CrossRef](#)]
19. Ruan, X.; Qu, S.-W.; Zhu, Q.; Ng, K.B.; Chan, C.H. A Complementary Circularly Polarized Antenna for 60-GHz Applications. *IEEE Antennas Wirel. Propag. Lett.* **2017**, *16*, 1373–1376. [[CrossRef](#)]
20. Lin, W.; Ziolkowski, R.W.; Baum, T.C. 28 GHz Compact Omnidirectional Circularly Polarized Antenna for Device-to-Device Communications in the Future 5G Systems. *IEEE Trans. Antennas Propag.* **2017**, *65*, 6904–6914. [[CrossRef](#)]
21. Wu, Z.; Miao, Z.; Deng, X. High-Gain and Wideband Circularly Polarized Endfire Leaky-Wave Antenna Array Based on the Complementary Dipole. *IEEE Trans. Antennas Propag.* **2023**, *71*, 6168–6172. [[CrossRef](#)]
22. Xu, J.; Luk, K.-M.; Hong, W. Low-Profile Wideband Circularly Polarized Complementary Antenna and Arrays for Millimeter-Wave Communications. *IEEE Trans. Antennas Propag.* **2023**, *71*, 2052–2063. [[CrossRef](#)]
23. Gatti, F.; Bozzi, M.; Perregrini, L.; Wu, K.; Bosisio, R.G. A novel substrate integrated coaxial line (SICL) for wide-band applications. In Proceedings of the 2006 European Microwave Conference, Manchester, UK, 10–15 September 2006; pp. 1614–1617.
24. Miao, Z.-W.; Hao, Z.-C. A Wideband Reflectarray Antenna Using Substrate Integrated Coaxial True-Time Delay Lines for QLink-Pan Applications. *IEEE Antennas Wirel. Propag. Lett.* **2017**, *16*, 2582–2585. [[CrossRef](#)]
25. Liu, B.; Ma, Y.; Zhao, R.R.; Xing, W.Q.; Guo, Z.J. A Novel Substrate-Integrated Coaxial Line Transverse Slot Array Antenna. *IEEE Trans. Antennas Propag.* **2019**, *67*, 6187–6192. [[CrossRef](#)]
26. Dai, X.; Li, A.; Luk, K.M. A Wideband Compact Magnetolectric Dipole Antenna Fed by SICL for Millimeter Wave Applications. *IEEE Trans. Antennas Propag.* **2021**, *69*, 5278–5285. [[CrossRef](#)]

**Disclaimer/Publisher’s Note:** The statements, opinions and data contained in all publications are solely those of the individual author(s) and contributor(s) and not of MDPI and/or the editor(s). MDPI and/or the editor(s) disclaim responsibility for any injury to people or property resulting from any ideas, methods, instructions or products referred to in the content.